Intraoperative CT augmentation for needle-based liver interventions

Sidaty El Hadramy, Juan Verde, Nicolas Padoy, Stéphane Cotin

Intraoperative CT augmentation for needle-based liver interventions

Sidaty El hadramy[1,2†], Juan Verde[3†], Nicolas Padoy[2,3], and Stéphane Cotin[1⋆]

[1] Inria, Strasbourg, France
[2] ICube, University of Strasbourg, Strasbourg, CNRS, France.
[3] IHU Strasbourg, Strasbourg, France

Abstract. This paper addresses the need for improved CT-guidance during needle-based liver procedures (i.e., tumor ablation), while reduces the need for contrast agent injection during such interventions. To achieve this objective, we augment the intraoperative CT with the preoperative vascular network deformed to match the current acquisition. First, a neural network learns local image features in a non-contrasted CT image by leveraging the known preoperative vessel tree geometry and topology extracted from a matching contrasted CT image. Then, the augmented CT is generated by fusing the labeled vascular tree and the non-contrasted intraoperative CT. Our method is trained and validated on porcine data, achieving an average dice score of 0.81 on the predicted vessel tree instead of 0.51 when a medical expert segments the non-contrasted CT. In addition, vascular labels can also be transferred to provide additional information. Source code of this work is publicly available at https://github.com/Sidaty1/Intraoperative_CT_augmentation.

Keywords: Liver tumor ablation · Needle-based procedures · Patient-specific interventions · CT-guidance · Medical image augmentation

1 Introduction

Needle-based liver tumor ablation techniques (e.g., radiofrequency, microwave, laser, cryoablation) have a great potential for local curative tumor control [1], with comparable results to surgery in the early stages for both primary and secondary cancers. Furthermore, as it is minimally invasive, it has a low rate of major complications and procedure-specific mortality, and is tissue-sparing, thus, its indications are growing exponentially and extending the limits to more advanced tumors [3]. CT-guidance is a widely used imaging modality for placing the needles, monitoring the treatment, and following up patients. However, it is limited by the exposure to ionizing radiation and the need for intravenous injection of contrast agents to visualize the intrahepatic vessels and the target tumor(s).

In standard clinical settings, the insertion of each needle requires multiple check points during its progression, fine-tune maneuvers, and eventual repositioning. This leads to multiple CT acquisitions to control the progression of the needle with respect

⋆ Corresponding author. E-mail: stephane.cotin@inria.fr
† These authors contributed equally to this work

to the vessels, the target, and other sensible structures [26]. However, intrahepatic vessels (and some tumors) are only visible after contrast-enhancement, which has a short lifespan and dose-related deleterious kidney effects. It makes it impossible to perform each of the control CT acquisitions under contrast injection. A workaround to shortcut these limitations is to perform an image fusion between previous contrasted and intraoperative non-contrasted images. However, such a solution is only available in a limited number of clinical settings, and the registration is only rigid, usually deriving into bad results. In this work, we propose a method for visualizing intrahepatic structures after organ motion and needle-induced deformations, in non-injected images, by exploiting image features that are generally not perceivable by the human eye in common clinical workflows.

To address this challenge, two main strategies could be considered: **image fusion** and **image processing** techniques. Image fusion typically relies on the estimation of rigid or non-rigid transformations between 2 images, to bring into the intraoperative image structures of interest only visible in the preoperative data. This process is often described as an optimization problem [9, 10] which can be computationally expensive when dealing with non-linear deformations, making their use in a clinical workflow limited. Recent deep learning approaches [11, 12, 14] have proved to be a successful alternative to solve image fusion problems, even when a large non-linear mapping is required. When ground-truth displacement fields are not known, state-of-the-art methods use unsupervised techniques, usually an encoder-decoder architecture [7, 13], to learn the unknown displacement field between the 2 images. However, such unsupervised methods fail at solving our problem due to lack of similar image features between the contrasted (CCT) and non-contrasted (NCCT) image in the vascular tree region (see section 3.3).

On the other hand, deep learning techniques have proven to be very efficient at solving image processing challenges [15]. For instance, image segmentation [16], image style transfer [17], or contrast-enhancement to cite a few. Yet, segmenting vessels from non-contrasted images remains a challenge for the medical imaging community[16]. Style transfer aims to transfer the style of one image to another while preserving its content [17–19]. However, applying such methods to generate a contrasted intraoperative CT is not a sufficiently accurate solution for the problem that we address. Contrast-enhancement methods could be an alternative. In the method proposed by Seo *et al.* [20], a deep neural network synthesizes contrast-enhanced CT from non contrast-enhanced CT. Nevertheless, results obtained by this method are not sufficiently robust and accurate to provide an augmented intraoperative CT on which needle-based procedures can be guided.

In this paper we propose an alternative approach, where a neural network learns local image features in a NCCT image by leveraging the known preoperative vessel tree geometry and topology extracted from a matching (undeformed) CCT. Then, the augmented CT is generated by fusing the deformed vascular tree with the non-contrasted intraoperative CT. Section 2 presents the method and its integration in the medical workflow. Section 3 presents and discusses the results, and finally we conclude in section 4 and highlight some perspectives.

2 Method

In this section, we present our method and its compatibility with current clinical workflows. A few days or a week before the intervention, a preoperative diagnostic multiphase contrast-enhanced image (MPCECT) is acquired (Fig. 1, yellow box). The day of the intervention, a second MPCECT image is acquired before starting the needle insertion, followed by a series of standard, non-injected acquisitions to guide the needle insertion (Fig. 1, blue box). Using such a non-contrasted intraoperative image as input, **our method performs a combined non-rigid registration and augmentation of the intraoperative CT** by adding anatomical features (mainly intrahepatic vessels and tumors) from the preoperative image to the current image. To achieve this result, our method only requires to process and train on the baseline MPCECT image (Fig. 1, red box). An overview of the method is shown in the Fig 2 and the following sections describe its main steps.

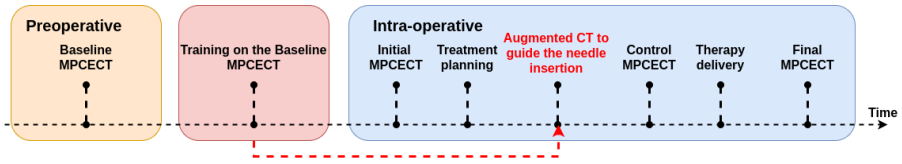

Fig. 1. Integration of our method in the clinical workflow. The neural network trained on preoperative MPCECT avoids contrast agent injections during the intervention.

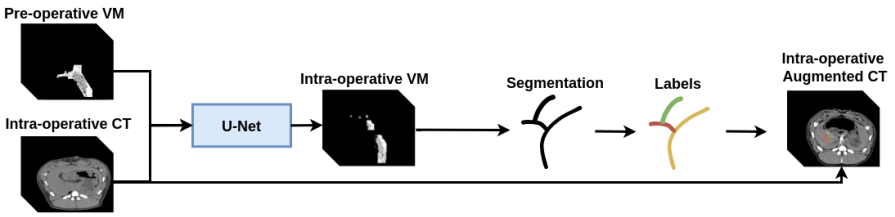

Fig. 2. The neural network takes as input the preoperative vessel map (VM) and the intraoperative NCCT, and outputs the intraoperative vessel map (VM) from which we extract the deformed vascular tree. Finally, the augmented CT is created by fusing the segmented image and labels with the intraoperative NCCT.

2.1 Vessel map extraction

We call Vessel Map (VM) the region of interest defining the vascular tree in the NCCT. Since vascular structures are not visible in non-contrasted images, the extraction of this map is done by segmenting the CCT and then using this segmentation as a mask in the NCCT. Mathematical morphology operators, in particular a dilation operation [23], are

performed on the segmented region of interest to slightly increase its dimensions. This is needed to compensate for segmentation errors and the slight anatomical motion that may exist between the contrasted and non-contrasted image acquisitions. In practice, the acquisition protocols limit the shift between the NCCT and CCT acquisitions, and only a few sequential dilation operations are needed to ensure we capture the true vessel fingerprint in the NCCT image. Note that the resulting vessel map is not a binary mask, but a subset of the image limited to the volume covered by the vessels.

2.2 Data augmentation

The preoperative MPCECT provides a couple of registered NCCT and CCT images. This is obviously not sufficient for training purposes, as they do not represent the possible soft tissue deformation that may occur during the procedure. Therefore, we augment the data set by applying multiple random deformations to the original images. Random deformations are created by considering a predefined set of control points for which we define a displacement field with a random normal distribution. The displacement field of the full volume is then obtained by linearly interpolating the control points' displacement field to the rest of the volume. All the deformations are created using the same number of control points and characteristics of the normal distributions.

2.3 Neural Network

Predicting the vascular tree location in the deformed intraoperative NCCT is done using a U-net [5] architecture. The neural network takes as input the preoperative vessel map and the intraoperative NCCT, and outputs the intraoperative vessel map. Our network learns to find the image features (or vessel fingerprint) present in the vessel map, in a given NCCT assuming the knowledge of its geometry, topology, and the distribution of contrast from the preoperative MPCECT. The architecture of our network is illustrated in figure 3. It consists of a four layers analysis (left side) and synthesis (right side) paths that provide a non-linear mapping between low resolution input and output images. Both paths include four 3x3x3 unpadded convolutions, each followed by a Leaky Rectified Linear Unit (LeakyReLU) activation function. The analysis includes a 2x2x2 max pooling with a stride of 1, while the synthesis follows each convolution by a 2x2x2 up-convolution with a stride of 1. Shortcut connections from layers of equal resolution in the analysis path provide the essential high-resolution features to the synthesis path. In the last layer, a 1x1x1 convolution reduces the number of output channels to one, yielding the vessel map in the intraoperative image. Our network is trained by minimizing the mean square error between the predicted and ground truth vessel map. Training details are presented in section 3.

2.4 Augmented CT

Once the network has been trained on the patient-specific preoperative data, the next step is to augment and visualize the intraoperative NCCT. This is done in 3 steps:

– The dilatation operations introduced in section 2.1 are not reversible (i.e. the segmented vessel tree cannot be recovered from the VM by applying the same number

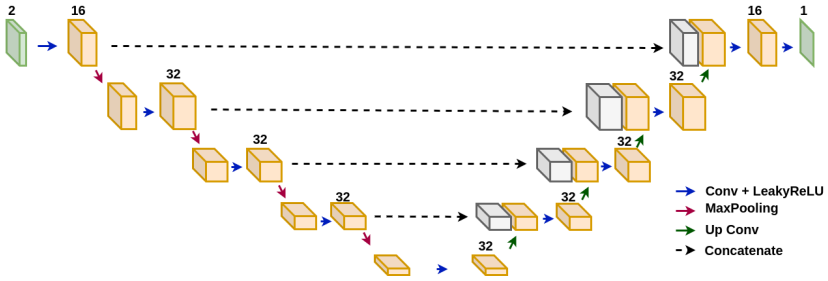

Fig. 3. Our neural network uses a four-path encoder-decoder architecture and takes as input a two-channel image corresponding to the intraoperative NCCT image concatenated with the preoperative vessel map. The output is the intraoperative vessel map.

of erosion operations). Also, neighboring branches in the vessel tree could end up being fused, thus changing the topology of the vessel map. Therefore, to retrieve the correct segmented (yet deformed) vascular tree, we compute a displacement field between the pre- and intraoperative VMs. This is done with the Elastix library [21, 22]. The resulting displacement field is applied on the preoperative segmentation to retrieve the intraoperative vessel tree segmentation. This is illustrated in figure 4.

– The augmented image is obtained by fusing the predicted intraoperative segmentation with the intraoperative NCCT image. The augmented vessels are displayed in green to ensure the clinician is aware this is not a true CCT image (see Fig. 5).
– It is also possible to add anatomical labels to the intraoperative augmented CT to further assist the clinician. To achieve this objective, we compute a graph data structure from the preoperative segmentation. We first extract the vessel centerlines as described in [4]. To define the associated graph structure, we start by selecting all branches with either no parent or no children. The branch with the highest radius is then selected as the root edge. An oriented graph is created using a Breadth First Search algorithm starting from the root edge. Nodes and edges correspond respectively to vessel tree bifurcations and branches. We use the graph structure to associate each anatomical label (manually defined) with a Strahler [6] graph ordering. The same process is applied to the predicted intraoperative segmentation. This makes it possible to correctly map the preoperative anatomical labels (e.g. vessel name) and display them on the augmented image.

3 Results and Discussion

3.1 Dataset and implementation details

To validate our approach, 4 couples of MPCECT abdominal porcine images were acquired from 4 different subjects. For a given subject, each couple corresponds to a preoperative and an intraoperative MPCECT. We recall that an MPCECT contains a set of registered NCCT and CCT images. These images are then cropped and down-sampled

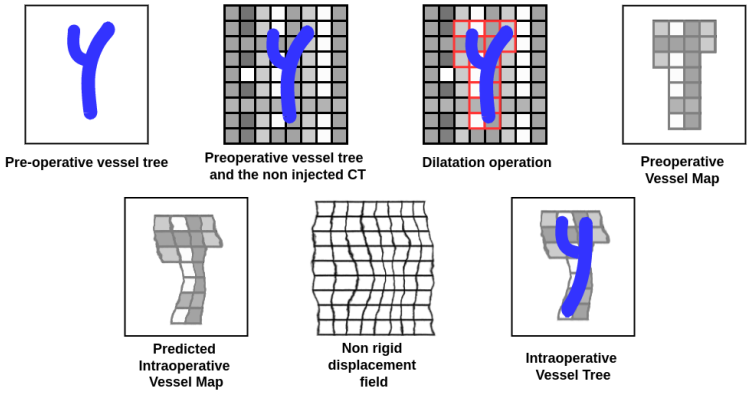

Fig. 4. This figure illustrates the different stages of the pipeline adopted to generate the VM and show how the vessel tree topology is retrieved from the predicted intraoperative VM by computing a displacement field between the preoperative VM and the predicted VM. This field is applied to the preoperative segmentation to get the intraoperative one.

to 256x256x256, and the voxels intensities are scaled between 0 and 255. Finally, we extract the VM from each MPCECT sample and apply 3 dilation operations, which demonstrated the best performance in terms of prediction accuracy and robustness on our data. We note that public data sets such as DeepLesion [24], 3Dircadb-01 [25] and others do not fit our problem since they do not include the NCCT images. Aiming at a patient-specific prediction, we only train on a "subject" at a time. For a given subject, we generate 100 displacement fields using the data augmentation strategy explained above with 50 voxels for the control points spacing in the three spatial directions and a standard deviation of 5 voxels for the normal distributions. The resulting deformation is applied to the **preoperative** MPCECT and its corresponding VM. Thus, we end up with a set of 100 triplets (NCCT, CCT and VM). Two out of the 100 triplets are used for each training batch, where one is considered as the pre-operative MPCECT and the other as the intraoperative one. This makes it possible to generate up to 4950 training and validation samples. The **intraoperative** MPCECT of the same subject is used to test the network. Our method is implemented in Tensorflow 2.4, on a GeForce RTX 3090. We use an Adam optimizer ($\beta_1 = 0.001$, $\beta_2 = 0.999$) with a learning rate of 10^{-4}. The training process converges in about 1,000 epochs with a batch size of 1 and 200 steps per epoch.

3.2 Results

To assess our method, we use a dice score to measure the overlap between our predicted segmentation and the ground truth. Being a commonly used metric for segmentation problems, Dice aligns the nature of our problem as well as the clinical impact of our solution. We ha performed tests on 4 different (porcine) data sets. Results are reported in table 1. The method achieved a mean dice score of 0.81. An example of a subject intraoperative augmented CT is illustrated in figure 5, where the three images correspond

respectively to the initial non injected CT, the augmented CT without and with labels. Figure 6 illustrates the results of our method for *Subject 1*. The green vessels correspond to the ground truth intraoperative segmentation, the orange ones to the predicted intraoperative segmentation and finally the gray vessel tree corresponds to the preoperative CCT vessel tree. Such results demonstrate the ability of our method to perform very well even in the presence of large deformations.

Dice score	Subject 1	Subject 2	Subject 3	Subject 4	Mean	Std
Ours	**0.8**	**0.77**	**0.79**	**0.90**	**0.81**	**0.04**
Expert clinician	**0.52**	**0.45**	**0.53**	**0.52**	**0.51**	**0.03**

Table 1. This table presents our results over 4 subjects in terms of dice score. For each subject the network was trained on the preoperative MPCECT and tested on the intraoperative MPCECT. We achieve a mean dice score of 0.81 vs. 0.51 for the clinical experts.

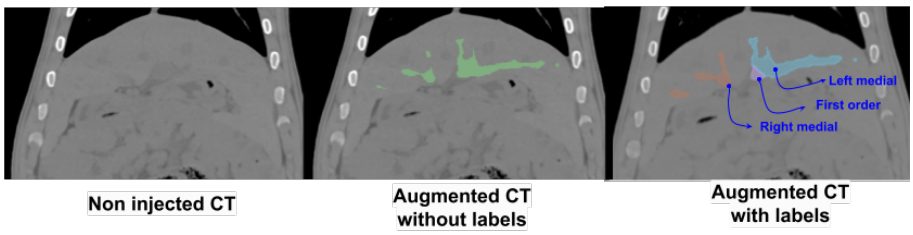

Fig. 5. In this figure we show the original NCCT on the left. The middle image shows the augmented CT with the predicted vessel tree (in green). The rightmost image shows the augmented image with anatomical labels transferred from the preoperative image segmentation and labelling.

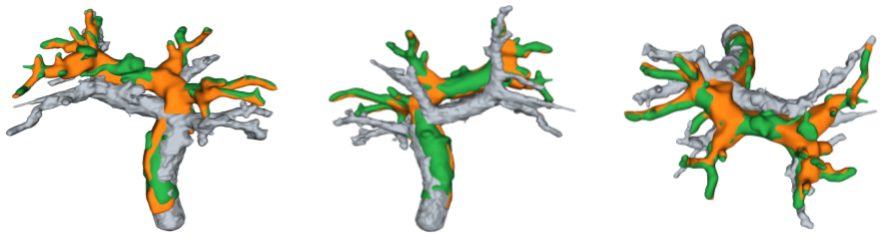

Fig. 6. Assessment of our method for Subject 1. We show 3 different views of the intraoperative vessel prediction (in orange), the ground truth (in green) and the preoperative vessels (in grey).

Qualitative assessment: To further demonstrate the value of our method, we have asked two clinicians to manually segment the NCCT images in the intraoperative MPCECT data. Their results (mean and standard deviation) are reported in table 1. Our method

outperforms the results of both clinicians, with an average dice score of 0.81 against 0.51 as a mean for the clinical experts.

3.3 Ablation study and additional results

Vessel map: We have removed the VM from the network input to demonstrate its impact on our results. Using the data of the $Subject1$, a U-net was trained to segment the vessel tree of the intraoperative NCCT image. The network only managed to segment a small portion of the main portal vein branch. Thus, achieving a dice score of **0.16** vs **0.79** when adding the preoperative VM as additional input. We also studied the influence of the diffusion kernel applied to the initial segmentation. We have seen, on our experimental data, that 3 dilation operations were sufficient to compensate for the possible motion between NCCT and CCT acquisitions.
Comparison with VoxelMorph: The problem that we address can be seen from different angles. In particular, we could attempt to solve it by registering the preoperative NCCT to the intraoperative one and then applying the resulting displacement field to the known preoperative segmentation. However, state-of-the-art registration methods such as VoxelMorph [7] and others do not necessarily guarantee a diffeomorphic [8] displacement field that ensures the continuity of the displacement field inside the parenchyma where the intensity is quite homogeneous on the NCCT. To assess this assumption, a VoxelMorph[†] network was trained on the $Subject1$ of our porcine data sets. We trained the network with both MSE and smoothness losses during 100 epochs and given a batch of size 4. Results are illustrated below in Figure 7. While the VoxelMorph network accurately registers the liver shape, the displacement field is almost null in the region of vessels inside the parenchyma. Therefore, the preoperative vessel segmentation is not correctly transferred into the intraoperative image.

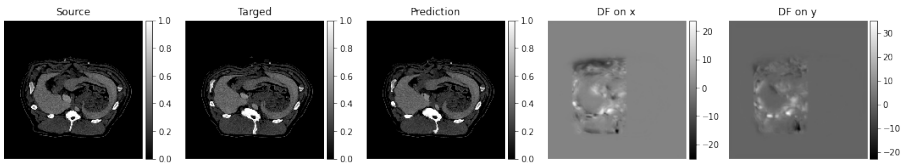

Fig. 7. Illustration of Voxelmorph registration between NCCT preoperative and intraoperative images. The prediction is the output of VoxelMorph method. DF stands for the displacement fields on x and y predicted by VoxelMorph method.

4 Conclusion

In this paper, we proposed a method for augmenting intra-operative NCCT images as a means to improve needle CT-guided techniques while reducing the need for contrast agent injection during tumor ablation procedures, or other needle-based procedures. Our

[†] https://github.com/voxelmorph/voxelmorph

method uses a U-net architecture to learn local vessel tree image features in the NCCT by leveraging the known vessel tree geometry and topology extracted from a matching CCT image. The augmented CT is generated by fusing the predicted vessel tree with the NCCT. Our method is validated on several porcine images, achieving an average dice score of 0.81 on the predicted vessel tree location. In addition, it demonstrates robustness even in the presence of large deformations between the preoperative and intraoperative images. Our future steps will essentially involve applying this method to patient data and perform a small user study to evaluate the usefulness and limitations of our approach.

5 Aknowledgments

This work was partially supported by French state funds managed by the ANR under reference ANR-10-IAHU-02 (IHU Strasbourg). The authors would like to thank Paul Baksic and Robin Enjalbert for proofreading the manuscript.

References

1. Izumi N, Asahina Y, Noguchi O, Uchihara M, Kanazawa N, Itakura J, Himeno Y, Miyake S, Sakai T, Enomoto N. Risk factors for distant recurrence of hepatocellular carcinoma in the liver after complete coagulation by microwave or radiofrequency ablation. Cancer. 2001 Mar 1;91(5):949-56. PMID: 11251946.
2. Lencioni R, Cioni D, Crocetti L, Franchini C, Pina CD, Lera J, Bartolozzi C. Early-stage hepatocellular carcinoma in patients with cirrhosis: long-term results of percutaneous image-guided radiofrequency ablation. Radiology. 2005 Mar;234(3):961-7.
3. Schullian P, Johnston EW, Putzer D, Eberle G, Laimer G, Bale R. Safety and efficacy of stereotactic radiofrequency ablation for very large (*gt* 8 cm) primary and metastatic liver tumors. Sci Rep. 2020 Jan 31;10(1):1618.
4. Antiga, L. and B. Ene-Iordache. Centerline computation and geometric analysis of branching tubular surfaces with application to blood vessel modeling. WSCG, 2003.
5. Ronneberger, O., Fischer, P. and Brox, T. U-net: Convolutional networks for biomedical image segmentation. In International Conference on Medical image computing and computer-assisted intervention 234–241 (Springer, Cham, 2015).
6. L. Devroye and P. Kruszewski. On the horton-Strahler number for random tries. Informatique théorique et Applications/Theoretical Informaties and Applications (vol. 30, n° 5, 1996, pp. 443-456).
7. Balakrishnan G, Zhao A, Sabuncu M R, Guttag J and Dalca A V 2019 VoxelMorph: a learning framework for deformable medical image registration IEEE Trans. Med. Imaging 38 1788–800
8. Cao Y, Miller MI, Winslow RL, Younes L. 2005. Large deformation diffeomorphic metric mapping of vector fields. IEEE Trans Med Imaging. 24(9):1216–1230
9. S. Klein, M. Staring, K. Murphy, M. A. Viergever, and J. P. Pluim, "Elastix: a toolbox for intensity-based medical image registration," IEEE transactions on medical imaging, vol. 29, no. 1, pp. 196–205, 2009
10. B. B. Avants, N. J. Tustison, G. Song, P. A. Cook, A. Klein, and J. C. Gee, "A reproducible evaluation of ants similarity metric performance in brain image registration," Neuroimage, vol. 54, no. 3, pp. 2033–2044, 2011.
11. Cao, X., Yang, J., Wang, L., Xue, Z., Wang, Q., Shen, D. (2018). Deep Learning Based Inter-modality Image Registration Supervised by Intra-modality Similarity. In: Shi, Y., Suk, HI., Liu, M. (eds) Machine Learning in Medical Imaging. MLMI 2018. Lecture Notes in Computer Science(), vol 11046. Springer, Cham.

12. X. Yang, R. Kwitt, M. Styner, and M. Niethammer, “Quicksilver: Fast predictive image registration–a deep learning approach,” NeuroImage, vol. 158, pp. 378–396, 2017.
13. B. Kim, D. H. Kim, S. H. Park, J. Kim, J.-G. Lee, and J. C. Ye, “Cyclemorph: Cycle consistent unsupervised deformable image registration,” Medical Image Analysis, vol. 71, 2021.
14. H. Sokooti, B. De Vos, F. Berendsen, B. P. Lelieveldt, I. Isgum, ˇand M. Staring, “Nonrigid image registration using multi-scale 3d convolutional neural networks,” in International Conference on Medical Image Computing and Computer-Assisted Intervention. Springer, 2017, pp. 232–239.
15. Suganyadevi, S., Seethalakshmi, V. and Balasamy, K. A review on deep learning in medical image analysis. Int J Multimed Info Retr 11, 19–38 (2022).
16. Ramesh K, Kumar GK, Swapna K, Datta D, Rajest SS. A Review of Medical Image Segmentation Algorithms. EAI Endorsed Trans Perv Health Tech. 2021 Apr.
17. Leon A Gatys, Alexander S Ecker, and Matthias Bethge. A neural algorithm of artistic style. arXiv preprint arXiv:1508.06576, 2015.
18. Leon A Gatys, Alexander S Ecker, and Matthias Bethge. Image style transfer using convolutional neural networks. In Proc. IEEE Conference on Computer Vision and Pattern Recognition (CVPR), 2016.
19. Justin Johnson, Alexandre Alahi, and Li Fei-Fei. Perceptual losses for real-time style transfer and super-resolution. In Proc. European Conference on Computer Vision (ECCV), pages 694–711. Springer, 2016
20. Minkyo Seo, Dongkeun Kim, Kyungmoon Lee, Seunghoon Hong, Jae Seok Bae, Jung Hoon Kim, and Suha Kwak "Neural Contrast Enhancement of CT Image," 2021 IEEE Winter Conference on Applications of Computer Vision (WACV), Waikoloa, HI, USA, 2021.
21. S. Klein, M. Staring, K. Murphy, M.A. Viergever, J.P.W. Pluim, "elastix: a toolbox for intensity based medical image registration," IEEE Transactions on Medical Imaging, vol. 29, no. 1, pp. 196 - 205, January 2010.
22. D.P. Shamonin, E.E. Bron, B.P.F. Lelieveldt, M. Smits, S. Klein and M. Staring, "Fast Parallel Image Registration on CPU and GPU for Diagnostic Classification of Alzheimer's Disease", Frontiers in Neuroinformatics, vol. 7, no. 50, pp. 1-15, January 2014.
23. R. M. Haralick, S. R. Sternberg and X. Zhuang, "Image Analysis Using Mathematical Morphology," in IEEE Transactions on Pattern Analysis and Machine Intelligence, vol. PAMI-9, no. 4, pp. 532-550, July 1987.
24. Yan K, Wang X, Lu L, Summers RM. DeepLesion: automated mining of large-scale lesion annotations and universal lesion detection with deep learning. J Med Imaging (Bellingham). 2018 Jul;5(3):036501. doi: 10.1117/1.JMI.5.3.036501. Epub 2018 Jul 20.
25. Soler, L., A. Hostettler, V. Agnus, A. Charnoz, J. Fasquel, J. Moreau, A. Osswald, M. Bouhadjar, and J. Marescaux. “3D image reconstruction for comparison of algorithm database: A patient specific anatomical and medical image database.” IRCAD, Strasbourg, France, Tech. Rep (2010).
26. Arnolli MM, Buijze M, Franken M, de Jong KP, Brouwer DM, Broeders IAMJ. System for CT-guided needle placement in the thorax and abdomen: A design for clinical acceptability, applicability and usability: System for CT-guided needle placement in the thorax and abdomen. Int J Med Robotics Comput Assist Surg. 2018 Feb;14(1):e1877